Cytokine 122 (2019) 154143

Contents lists available at ScienceDirect

Cytokine

journal homepage: www.elsevier.com/locate/cytokine

TRAF6: A player in CVB3-induced myocarditis?

Oana N. Ursu[a,b], Tina Beyer[a,b,1], Martina Sauter[b], Annunziata Fragasso[a], Sandra Bundschuh[b], Karin Klingel[b,2], Barbara Munz[a,*,2]

[a] University Hospital Tübingen Medical Clinic, Department of Sports Medicine, Hoppe-Seyler-Str. 6, D-72076 Tübingen, Germany
[b] University Hospital Tübingen, Department of Molecular Pathology, Institute for Pathology and Neuropathology, Liebermeisterstr. 8, D-72076 Tübingen, Germany

ARTICLE INFO

Keywords:
TRAF6
CVB3
Myocarditis
HeLa cells
NFkappaB

ABSTRACT

Coxsackievirus B3 (CVB3) is an important inducer of myocarditis, which, in susceptible individuals, can chronify and eventually lead to the development of dilated cardiomyopathy and heart failure. The respective mechanisms are not completely understood. Here, we analyzed expression of the *TRAF6* gene, encoding TNF receptor-associated factor 6 (TRAF6), a signal transduction scaffold protein that acts downstream of cytokine receptors, in heart tissue of susceptible and non-susceptible mouse strains. We found that after infection, *TRAF6* expression was upregulated in both non-susceptible C57BL/6 wildtype and susceptible A.BY/SnJ and C57BL/6-TLR3 (−/−) mice, however, to different degrees. In infected HeLa cells, we also found moderately elevated TRAF6 levels after infection, in addition, activity of the transcription factor nuclear factor kappa B (NFκB), which can be activated downstream of TRAF6, was strongly enhanced in infected cells. To functionally analyze the role of TRAF6 with regard to infection progression, *TRAF6* expression was knocked down in cultured HeLa cells using specific siRNAs. We found that reduction of *TRAF6* expression had no effect on NFκB activation in response to infection. Taken together, our data suggest that CVB3 infection enhances TRAF6 levels, however, this induction might not be necessary for infection-induced NFκB activation.

1. Introduction

Coxsackievirus B3 CVB3) infection is a common cause of both acute and chronic myocarditis. After acute infection, certain patients undergo rapid virus clearance, which leads to complete recovery, whereas in others, virus persistence, leading to chronic infection, occurs (for review, see [9]). The reasons for these different progression patterns, which can be observed in both human patients and susceptible/non-susceptible mouse strains, are complex and have not completely been elucidated so far. On the one hand, immunological characteristics play a role, on the other hand, cardiomyocyte-specific factors appear to be important, specifically, activation of certain signal transduction pathways in these cells (for review, see [17]).

Several intrinsically susceptible mouse strains, such as A.BY/SnJ mice, are known. Furthermore, specific individual genetic modifications can render mice susceptible for virus persistence or chronic infection: Mice deficient in TLR3 and its adapter protein TRIF (Toll/IL-1 receptor domain-containing adapter inducing interferon-beta) are more susceptible to infection [19], whereas knocking out the *MyD88* gene, encoding another adapter protein interacting with all TLRs besides TLR3, leads to a higher degree of resistance [5]. Consistently, we could show that TLR3 is essential for the activation of dendritic cells and the early immunological response to CVB3 infection [22].

TNFR (tumor necrosis factor receptor)-associated factor 6 (TRAF6) is an intracellular scaffolding protein that directly and indirectly associates with various receptors of the TNFR- and interleukin-1 receptor-/toll-like receptor- (IL-1R/TLR) superfamilies. Upon binding to activated receptor complexes, TRAF6 initiates downstream signaling, specifically the activation of the transcription factor NFκB (nuclear factor kappa B) (for review, see [15,3]).

In CVB3-infected HeLa cells, NFκB is activated and appears to act in an anti-apoptotic manner, eventually promoting survival of infected cells and virus replication [4,16]. A predominantly cytoprotective function of NFκB has also been observed for other forms of cardiomyopathy, such as in myocardial inflammation induced by ischemia-reperfusion [1]. However, other authors observed no NFκB activation in response to CVB3 infection, but cleavage of IκBα by the viral protease $3C^{pro}$, which inhibits NFκB transactivation and enhances apoptosis [23,20].

With respect to the *in vivo* situation, most recently, some authors

* Corresponding author.
E-mail address: barbara.munz@med.uni-tuebingen.de (B. Munz).
[1] Present address: Medical Proteome Center, Institute for Ophthalmic Research, University of Tübingen, Nägelestrasse 5, D-72074 Tübingen, Germany.
[2] Both authors contributed equally to this work.

http://dx.doi.org/10.1016/j.cyto.2017.08.023
Received 14 March 2017; Received in revised form 11 August 2017; Accepted 28 August 2017
Available online 06 September 2017

could describe induction of NFκB activity in CVB3-infected murine hearts and a protective effect of NFκB inhibition using various approaches [6,24–25,21]. In addition, induction of *TRAF6* gene expression after infection has been demonstrated, and blockade of this induction also appears to have a beneficial effect [2].

Taken together, these data suggest that TRAF6 might be a regulator of NFκB activation patterns in response to CVB3 infection.

Here, we analyzed *TRAF6* expression patterns in susceptible, specifically A.BY/SnJ and TLR3(−/−), and non-susceptible mouse strains. In addition, we knocked down *TRAF6* and *NFκB* expression *in vitro* and analyzed the respective effects after CVB3 infection.

2. Materials and methods

2.1. Animals

A.BY/SnJ (A.BY-H2^{b} H2-T18^{f}/SnJ) and TLR3$^{-/-}$ on a C57BL/6 background (B6; 129S1-Tlr3^{tm1Flv}/J) mice were originally purchased from Jackson Laboratories (Bar Harbor, ME). Breeding colonies of these animals were maintained at the Department of Immunology, University of Tübingen, in a specific-pathogen-free animal facility. C57BL/6 (C57BL/6NCrl *H-2*^{b}) mice were purchased from Charles River (Sulzfeld, Germany). At the indicated time points, mice were sacrificed, cardiac tissue was dissected, and either fixed in 4% paraformaldehyde and embedded in paraffin for subsequent histological analysis or snap-frozen in liquid nitrogen and stored at −80 °C for RNA or protein isolation. All animal experiments were carried out in accordance with the German animal protection law (Regierungspräsidium Tuebingen, PA2/10).

2.2. Virus and animal infection procedures

CVB3 Nancy strain) was grown and propagated in Vero cells as previously described [10]. Virus titers were determined by an agar overlay plaque assay. For infection, four- to five-week-old mice were i.p. injected with 1×10^5 pfu CVB3 as described [10].

2.3. Tissue culture

Human HeLa cells were cultured in Dulbecco's modified Eagle's medium containing 10% fetal bovine serum at 37 °C and 5% CO_2. For all infection experiments, cells were serum-starved overnight and subsequently CVB3-infected for 4 h with an MOI of 5. At the time of harvesting, 5–10% of the cells were VP1-positive in all experiments.

2.4. Transfection with specific siRNAs

siRNA transfection was carried out using predesigned, specific siRNAs purchased from Sigma. For knockdown of *TRAF6* expression, two different, unrelated siRNA species were employed in parallel to rule out off-target effects:

TRAF6 siRNA-1: sense: 5′-GAGACAUCUUGAGGAUCAU[dT][dT]-3′, antisense: 5′-AUGAUCCUCAAGAUGUCUC[dT][dT]-3′;

TRAF6 siRNA-2: sense: 5′-CAAAGUUGCUGAAAUCGAA[dT][dT]-3′, antisense: 5′-UUCGAUUUCAGCAACUUUG[dT][dT]-3′,

NFκB p65 siRNA-1: sense: 5′-GGAAUCCAGUGUGUGAAGA[dT][dT]-3′,

antisense: 5′-UCUUCACACACUGGAUUCC[dT][dT]-3′. As a negative control, a non-gene-specific, commercially available "scrambled" siRNA (Santa Cruz Biotechnology) was employed. HeLa cells were transfected using the XtremeGene siRNA transfection reagent (Roche) according to the manufacturer's instructions.

2.5. RNA isolation and qPCR

RNA isolation from murine hearts was performed using the AllPrep kit (Qiagen) or the NucleoSpin RNA kit (Macherey-Nagel). Semi-quantitative real time PCR analysis was carried out using the iCycler MyiQ system (Bio-Rad). Gene expression was analyzed using the Eva Green Mastermix (Bio-Rad). For detection of different transcripts, the following primers were used: mIL-6 sense 5′-AATCAGAATTGC CATTGCACAA -3′, antisense 5′-ACAAGTCGGAGGCTTAATTACACAT-3′, hIL-6 sense 5′-GAGTAGTGAGGAACAAGCCAGA-3′, antisense 5′-CATTT GTGGTTGGGTCAGGG-3′, mTraf6 sense 5′-GCGAGAGATTCTTTC CCTGACG-3′, antisense 5′-TTGGCACTGGGGACAATTCAC-3′, hTRAF6 sense 5′-AGTTTGACCCACCCCTGGAAAG-3′, antisense 5′-GGACATTT GTGACCTGCATCCC-3′, mIL-1β sense 5′-GACGGACCCCAAAAGATG AAG-3′, antisense 5′-CAATGAGTGATACTGCCTGCC-3′, hNF-κB sense 5′-ACAAGTGGCCATTGTGTTCC-3′, antisense 5′-ACGTTTCTCC TCAATCCGGT-3′. In each experiment, melting curve analysis was performed to verify that a single transcript was produced. RT-qPCR relative gene expression was calculated using the comparative CT ($2^{-\Delta\Delta C}{}_{T}$) method, where expression was normalized to HPRT. Non-RT- and non-template controls were run for all reactions. Unless otherwise specified, data from at least three independent experiments were expressed as means ± S.D., $n = 3–5$. Significance was accepted at $P < 0.05$.

2.6. Immunofluorescence and Western blot analysis

Immunofluorescence and Western blot analyses were carried out as previously described [18]. Signal intensity was quantified using the ImageJ program (Wayne Rasband). The following antibodies were used for immunoblotting: rabbit anti-IκBα (1:200, Santa Cruz Biotechnology), rabbit anti-TRAF6 (1:2000, Millipore), rabbit anti-beta-tubulin (1:5000, Abcam). All immunoblots were performed at least three times, and, in case of the siRNA experiments, with samples from at least three independent transfections. For immunofluorescence, the following primary antibodies were used: rabbit anti-TRAF6 (1:100, Santa Cruz Biotechnology), goat anti-NF-κB p65 (1:100, Santa Cruz Biotechnology) and mouse anti-VP1 Cox mAB 31A2 (1:400, Mediagnost, Germany). The fluorescence-coupled secondary antibodies were Alexa594 donkey anti-rabbit, Alexa594 donkey anti-goat and Alexa488 donkey anti-mouse, all diluted 1:500 in PBS. For nuclear stain, the RedDot2 (a far-red dye, used in blue pseudocolor) was used.

2.7. Cytotoxicity assay

Cytotoxicity assays were performed with the Cytotoxicity Detection Kit^{Plus} (Roche), which measures the release of lactate dehydrogenase (LDH) into the cell culture supernatant upon damage of the plasma membrane via a coupled enzymatic reaction. Briefly, 100 µl of cell culture supernatant were incubated with 100 µl reaction mixture (containing the Catalyst and the Dye substrate mixture) for 30′, at RT and protected from light. The assay was terminated by adding Stop Solution, followed by reading the absorbance (ELISA reader) at 490 nm with a parallel reading at 600 nm as a reference. Background controls, as well as "low" and "high" controls, were included to determine LDH activity in the assay medium, LDH release from untreated, normal cells, and the maximal amount of "releasable" LDH activity in the cells. Experiments were done in triplicates or more. Cytotoxicity was determined by subtracting the absorbance value obtained with the background control from the average absorbance value of samples and controls, followed by calculating "% cytotoxicity" from the "high" control (minus background) by using the formula (exp value – "low" control)//("high" control – "low" control).

3. Results

3.1. TRAF6 expression after CVB3 infection in vivo

TRAF6 expression was analyzed by Western blot in cardiac tissue of

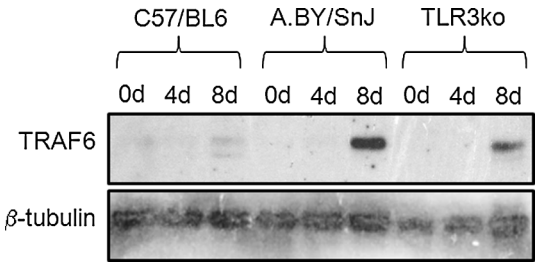

Fig. 1. Expression of the *TRAF6* gene in cardiac tissue of susceptible and non-susceptible mice after CVB3 infection. Representative Western blot analysis of TRAF6 protein concentrations in cardiac tissue of the three different mouse strains (uninfected, 4 d and 8 d p.i.). Analysis of β-tubulin concentrations served as a loading control.

the susceptible mouse strains A.BY/SnJ and C57BL/6-TLR3(−/−) before infection, and 4 d as well as 8 d after CVB3 infection. As a control, non-susceptible, wild-type C57BL/6 mice were used. Efficiency of infection was analyzed histologically (data not shown). As shown in Fig. 1, we found *TRAF6* induction at the protein level in all three mouse strains 8 d p.i., with induction being most prominent in strain A.BY/SnJ, followed by the also-susceptible C57BL/6-TLR3(−/−) mice, and weak in the non-susceptible C57BL/6 wildtype mice.

3.2. NFκB activity after CVB3 infection in vivo

To study NFκB activity in heart tissue in response to CVB3 infection, we analyzed protein concentrations of the NFκB inhibitor IκBα via Western blot. As shown in Fig. 2, there were no statistically significant differences with regard to IκBα levels, indicating comparable NFκB overall activity, in uninfected heart tissue of all three mouse strains. In response to CVB3 infection, we also found unaltered IκBα concentrations, indicating similar NFκB activity, in all mouse strains.

3.3. TRAF6 expression after CVB3 infection in vitro

To analyze the effects of CVB3 infection in a cell-homogenous and defined *in vitro* model system, excluding the potential effects of invading immune cells, cultured HeLa cells were CVB3-infected and TRAF6 levels and intracellular localization were studied via immunofluorescence. As shown in Fig. 3A, using this approach, we found an altered subcellular localization of the TRAF6 protein after infection: The protein appeared to be more diffusely distributed all over the cytoplasm when compared to controls, where it was predominantly concentrated in a specific region next to the nucleus. This phenomenon was not only visible in the infected cells themselves, but also in most other, VP1-negative cells, indicating paracrine, indirect effects. Similar results were obtained when stimulating the cells with TNFα (Fig. 3A). In addition, *TRAF6* expression was studied at both the protein and the mRNA level. As shown in Fig. 3B, we could detect a moderate induction of *TRAF6* expression in response to infection. A similar trend was also observed after TNFα treatment, even though the data did not reach statistical significance. The RNA data (Fig. 3C), by contrast, show a decrease in *TRAF6* expression after CVB3 infection. This is most likely due to the kinetics of TRAF6 mRNA and protein concentrations in the infected cells: Whereas TRAF6 protein is still high, the respective RNA might already start to degrade in the (dying) cells. When treating the cells with poly(I:C) to mimick viral infection, we also found upregulation of *TRAF6* expression (data not shown).

3.4. NFκB activity after CVB3 infection in vitro

Next, NFκB activity after CVB3 infection was studied. When analyzing NFκB p65 distribution in infected cells using immunofluorescence, we could detect high levels of nuclear p65 protein in VP1-positive and also in some VP1-negative cells, indicating strong NFκB activation in these cells. NFκB activation in VP1-negative cells might reflect paracrine effects of the infected cells or these cells might represent early-infected cells themselves. Overall, the results indicate major NFκB activation after infection (Fig. 4A). In addition, IκBα levels in infected HeLa cells were determined by Western blot. Using this approach, we could detect decreased IκBα levels after infection, suggesting enhanced NFκB activity. As a positive control for NFκB activation, cells were also stimulated with TNFα (Fig. 4A and B).

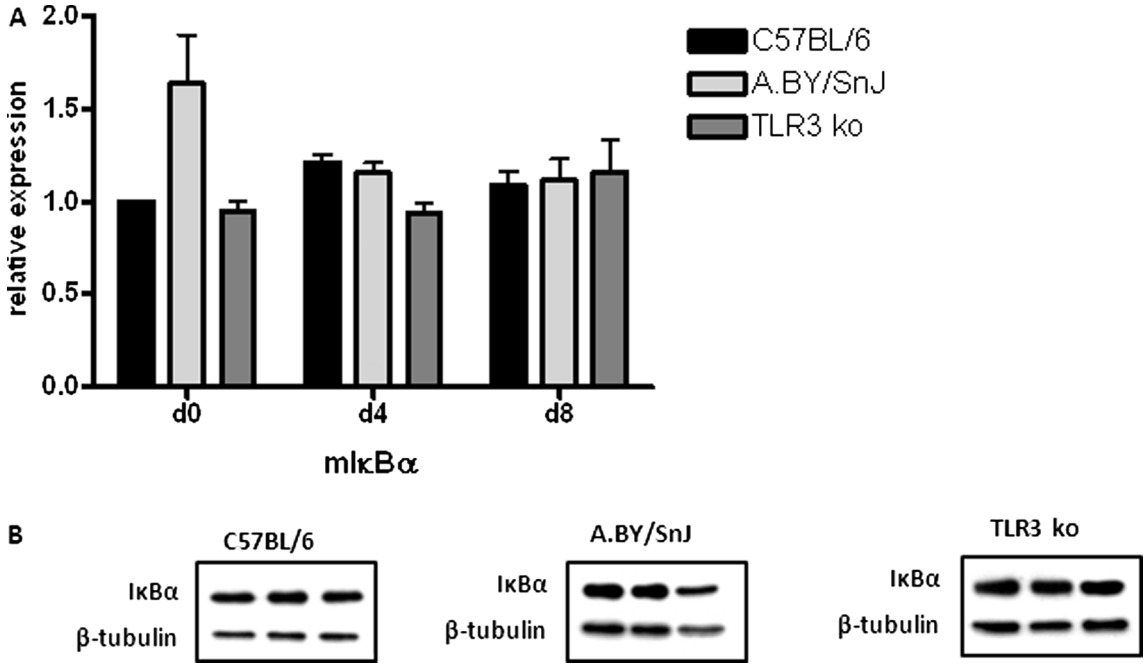

Fig. 2. IκBα protein levels in cardiac tissue of susceptible and non-susceptible mice after CVB3 infection. (A) IκBα protein levels were analyzed by Western blot in the three mouse strains before and 4 and 8 days after infection. Data are displayed as means ± SD. Relative expression was normalized to C57BL/6, d0. (B) Representative Western blots for the bar graphs shown in (A).

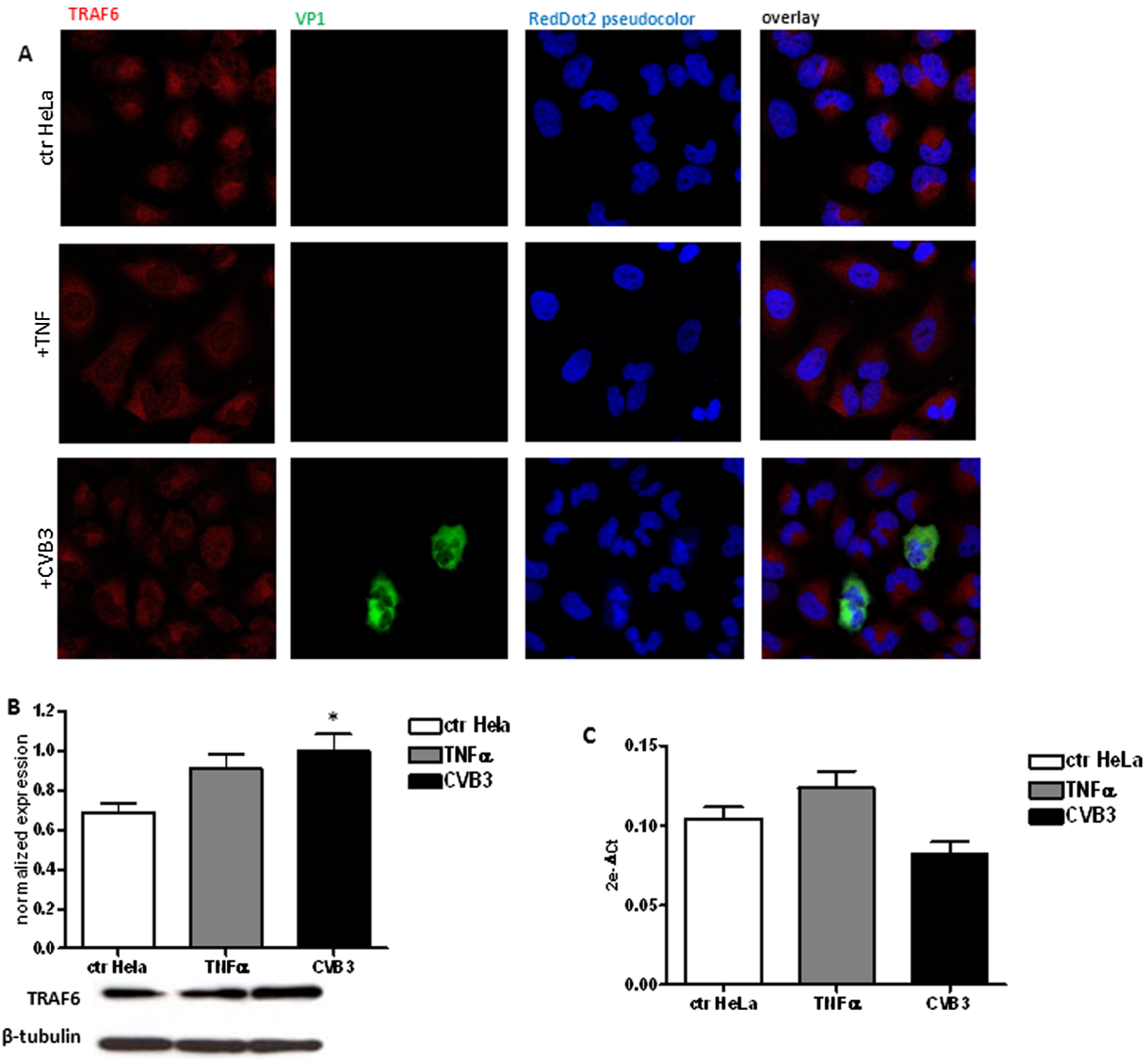

Fig. 3. *In vitro* analysis of *TRAF6* expression after CVB3 infection. (A) TRAF6 immunofluorescence analysis in TNFα-treated or CVB3-infected HeLa cells. (B) Representative TRAF6 immunoblot and densitometric analysis of five independent experiments after TNFα treatment or CVB3 infection; data were normalized to β-tubulin ($^{*}p: < 0.05$ vs. ctr HeLa cells). (C) TRAF6 mRNA concentrations in HeLa cells normalized to HPRT mRNA concentrations as assessed by qPCR. In all experiments, TNFα was kept on cells for 30 min; cells were infected with CVB3 for 4 h.

3.5. CVB3 infection and NFκB activation after knockdown of TRAF6 expression

To study the effects of TRAF6 on the course of CVB3 infection, expression of this gene was knocked down in cultured HeLa cells employing specific siRNAs. Using this approach, we achieved an approximately 50% reduction of *TRAF6* expression (Fig. 5A). After subsequent CVB3 infection, immunofluorescence analysis showed no reduction of NFκB nuclear translocation and thus activation when compared to untransfected or scr-transfected controls (Fig. 5B and data not shown), indicating that reducing *TRAF6* expression does not weaken CVB3-induced NFκB activation.

3.6. CVB3 infection and progression of infection after reduction of NFκB activity

To analyze progression of the infection process under conditions of reduced NFκB concentrations, we knocked down *p65* expression in HeLa cells using specific siRNAs. As shown in Fig. 6A, using this approach, we achieved an approximately 50% reduction of *p65* expression. After subsequent CVB3 infection, despite overall lower NFκB levels in the siRNA-transfected cells, nuclear translocation of this protein in infected cells could nevertheless be observed. In addition, infected cells, and, at lower levels, also their immediate neighbours, were characterized by a slightly enhanced p65 IF signal, indicating that CVB3 infection in part overpowers p65 silencing (Fig. 6A). The fact that we still observed reduced *p65* expression after CVB3 infection (Fig. 6A) does not rule out this hypothesis, since only approximately 5–10% of the cells were VP1-positive. Also, NFκB activity corresponds to nuclear translocation, but not necessarily to total *p65* gene expression at the RNA or at the protein level. Finally, we found that p65 silencing did not diminish the rate of CVB3-induced cell death when compared to untransfected or scr-transfected controls (Fig. 6B and data not shown). These data suggest that siRNA-mediated blocking of *p65* expression does not ameliorate CVB3-induced cytotoxicity.

4. Discussion

Our data indicate that after CVB3 infection, *TRAF6* expression is induced in hearts of both the non-susceptible mouse strain C57BL/6

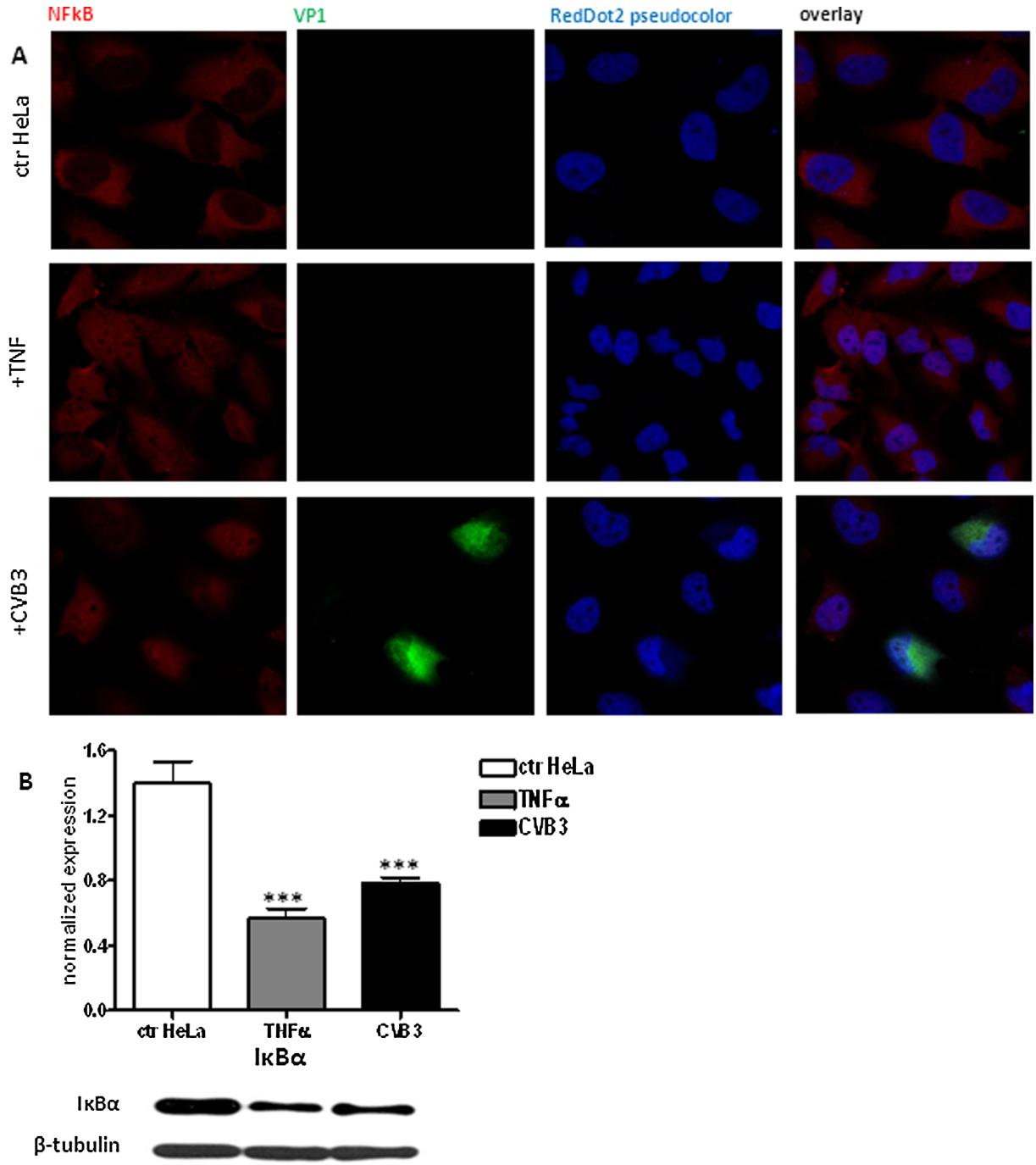

Fig. 4. *In vitro* analysis of NFκB activity after CVB3 infection. (A) NFκB immunofluorescence analysis of TNFα- treated or CVB3-infected HeLa cells. (B) Representative IκBα immunoblot of whole cell lysates and densitometric analysis of five independent experiments. Data were normalized against β-tubulin (***: $p < 0.001$ *vs.* ctr HeLa cells). For all experiments, TNFα was kept on cells for 30 min; cells were infected with CVB3 for 4 h.

and the susceptible strains A.BY/SnJ and C57BL/6-TLR3(-/-). Interestingly, Chen et al. [2], could also demonstrate induction of *TRAF6* gene expression at the mRNA and at the protein level in CVB3-infected hearts of BALB/c mice, another highly susceptible strain. In addition, recent data demonstrate that TRAF6 levels are increased in cardiac hypertrophy [7].

Elevated TRAF6 levels might be due to a high degree of *TRAF6* expression in invading immune cells. Consistently, induction was less pronounced in non-susceptible C57/BL6 mice when compared to the two susceptible mouse strains, possibly due to the more rapid clearance of the inflammatory infiltrate in C57/BL6 mice. In general, differences in *TRAF6* expression kinetics most likely reflect, at least in part, strain-specific immunological differences [10–12,22,13]. Regarding the C57BL/6-TLR3(−/−) mice, the fact that TRAF6 is a positive regulator of TLR3 signalling [8,14] might contribute to infection-induced *TRAF6* upregulation via an as yet unknown compensatory mechanism.

TRAF6 can also be differentially polyubiquitinylated and recent data suggest a central role of this process in CVB3-induced NFκB activation[6], thus, it might also be interesting to specifically analyze TRAF6's polyubiquitinylation pattern after CVB3 infection, specifically in susceptible versus non-susceptible mouse strains.

When analyzing IκBα concentrations in infected heart tissue, we found no major regulation. In addition, IκBα levels did not differ significantly between the different mouse strains. It should be mentioned

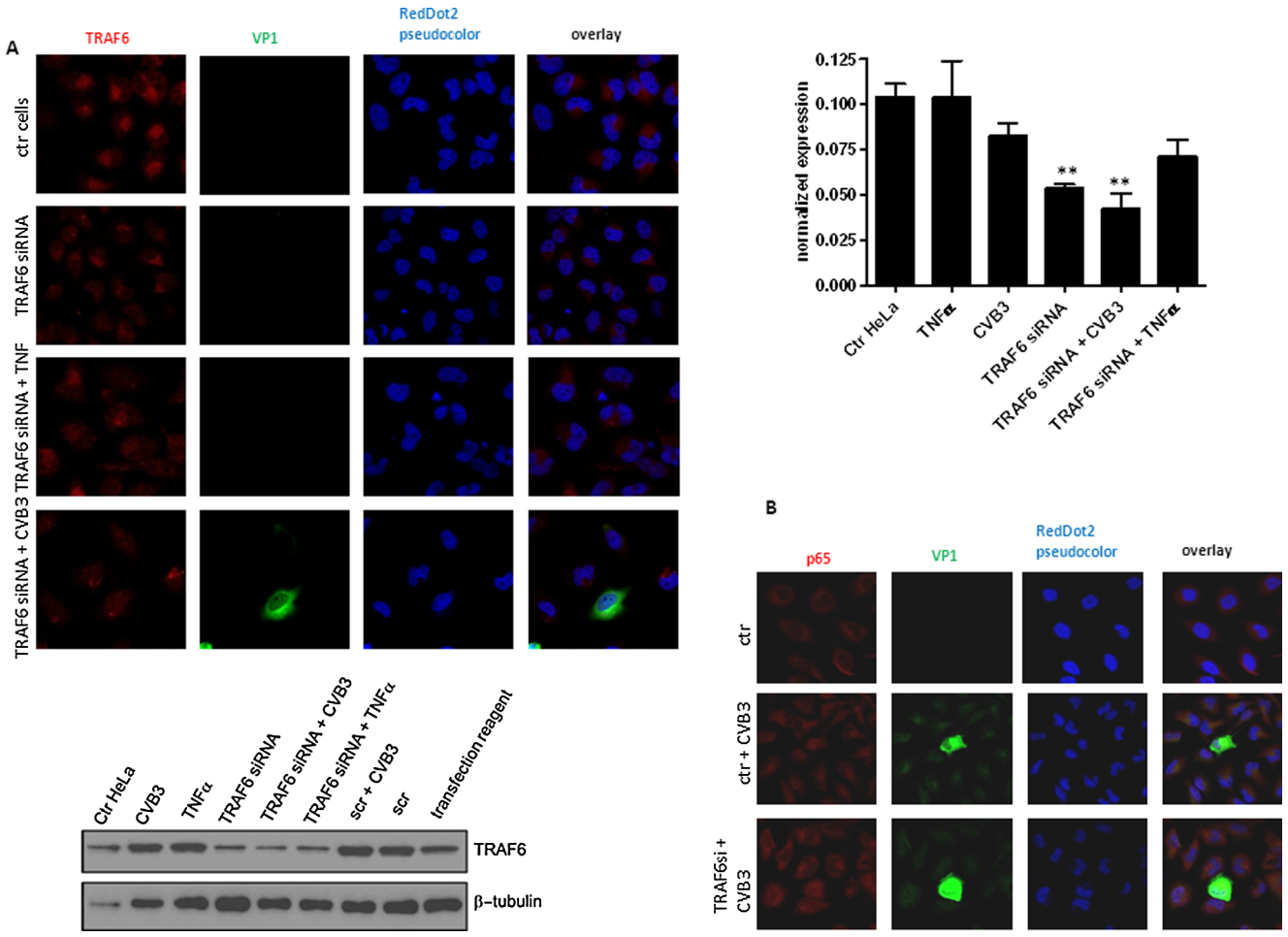

Fig. 5. Knockdown of *TRAF6* expression and CVB3 infection. (A) Immunofluorescence (top left panel), Western blot (bottom left panel) and qPCR (top right panel) determination of *TRAF6* expression in HeLa cells that had been transfected with TRAF6-specific siRNA with and without CVB3 infection or TNFα stimulation as indicated (**: $p < 0.01$ *vs.* ctr HeLa). (B) Immunofluorescence analysis of p65 distribution in infected HeLa cells after reduction of *TRAF6* expression.

here that some authors could describe induction of NFκB activity in CVB3-infected murine hearts [6,24–25,21]. This is likely to be due to the use of a different mouse strain (Balb/c) by these authors, in addition, different time points of analysis, different virus batches, or other differences with regard to the experimental setting might be responsible.

In an *in vitro* model system of CVB3-infected HeLa cells, we also found enhanced TRAF6 levels and an altered subcellular localization of this protein after infection, indicating that infection itself might affect TRAF6 production and trafficking. Interestingly, the altered subcellular TRAF6 distribution, specifically a nuclear-to-cytosolic translocation and an overall more diffuse staining pattern, was visible in almost all cells, not only in the VP1-positive, obviously infected cells. This might be due to paracrine effects of the infected cells, such as the release of growth factors and cytokines, which might influence TRAF6 trafficking in neighbouring cells.

When analyzing IκBα levels by Western blot in infected HeLa cells, we found a modest downregulation. This is consistent with the data presented by Esfandirei et al. [4], whereas Zarazoga et al. [23], and Saura et al. [20], observed no differences in overall IκBα levels after infection. These differences might be due to variations in the experimental settings, specifically timing and infection efficiency.

In addition, we analyzed NFκB p65 intracellular localization after infection by immunofluorescence. Here, we observed a clear nuclear translocation of this protein in infected cells, indicating strong NFκB activation. This is consistent with the data presented by other authors [4,23,20]. Interestingly, NFκB activation was again not only observed in the VP1-positive, clearly infected cells, but also in some VP1-negative cells. As stated above for TRAF6, this might again be due to paracrine effects of the infected cells. Alternatively, these cells might represent early-infected cells, in which the VP1 signal might not yet be detectable.

Nevertheless, the NFκB activation/deactivation pattern in response to infection has been and still is controversially discussed: Whereas Zarazoga et al. [23], and Saura et al. [20], claim IκBα cleavage by the viral protease $3C^{pro}$, resulting in inhibition of NFκB transactivation despite nuclear translocation, the data presented by Esfandiarei et al. [4], suggest enhanced NFκB activity after infection.

After reduction of *TRAF6* expression, we still found NFκB activation in response to viral infection, suggesting that activation of this transcription factor might occur independently of TRAF6. However, obviously, it is possible that reduced levels of this protein are still sufficient to achieve maximal NFκB activation, especially since we never achieved a more than 70% knockdown (50% on average) of *TRAF6* expression in our experiments. Interestingly, CVB3-induced cytotoxicity was also not ameliorated, but rather enhanced after knockdown of *TRAF6* expression (data not shown). Similarly, after transfection with a p65 siRNA and subsequent infection, there was no improvement of CVB3-induced cytotoxicity. This might be due to the fact that despite overall lower p65 levels, we could still observe nuclear translocation (and possibly also higher p65 levels in infected cells when compared to uninfected ones) of this protein in infected cells, suggesting that CVB3 infection "overpowers" siRNA-mediated p65 silencing. However, obviously, it is also possible that due to the high degree of overall

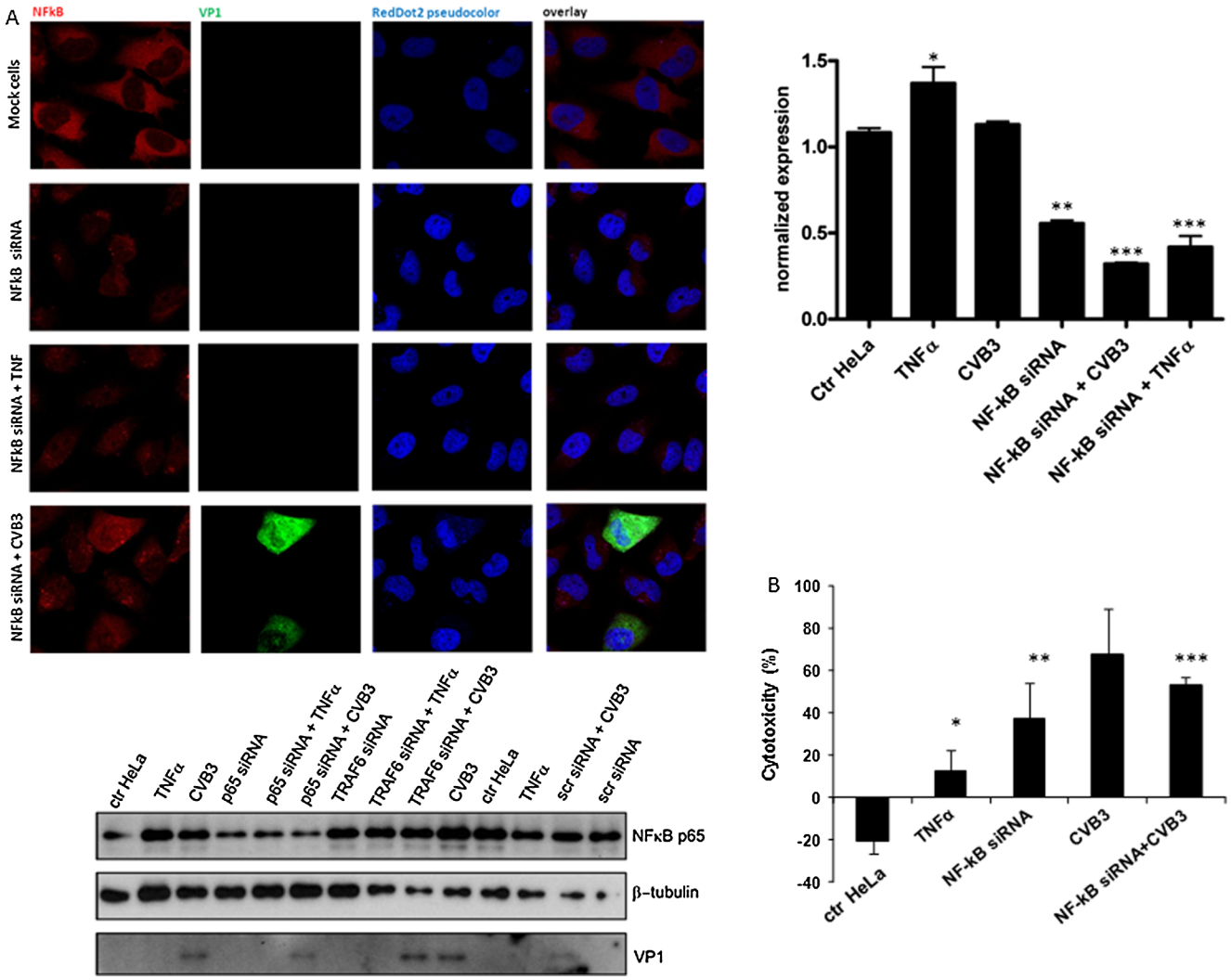

Fig. 6. Reduced NF-κB activity and CVB3 infection. (A) Immunofluorescence (top left panel), Western blot (bottom left panel) and qPCR (top right panel) analysis of *p65* expression after siRNA-mediated knockdown, with and without CVB3 infection or TNFα stimulation of the cells (*: $p < 0.05$, **: $p < 0.01$, ***: $p < 0.001$ *vs.* ctr HeLa). (B) Quantification of infection-associated cytotoxicity after knocking down *p65* expression. The negative value obtained with the control HeLa cells results from an average absorbance reading slightly lower than the "low" (background) control in the assay (*: $p < 0.05$, **: $p < 0.01$, ***: $p < 0.001$ *vs.* ctr HeLa).

cytotoxicity (approximately 70%) induced by CVB3 infection in our experiments, potential subtle effects of p65 silencing might have been missed.

5. Conclusions

Different degrees of *TRAF6* induction in susceptible and non-susceptible mouse strains, along with data generated by other authors suggesting a protective effect of TRAF6 and NFκB inhibition against the effects of virus-induced myocarditis, suggest that both factors are major players in this process. Interestingly, however, TRAF6 might not be crucial for CVB3-induced NFκB activation. In the future, it will be interesting to determine in more detail if and how TRAF6 influences CVB3-induced cardiac damage. Specifically, it will be interesting to perform analyses in further model systems, such as in TRAF6(−/−) cells, in cells harboring a recombinant, dominant-negative TRAF6 protein, or, most interestingly, in (cardiomyocyte-specific) TRAF6-deficient mice.

Acknowledgements

This project was specifically funded by a grant from the Friede-Springer-Herz-Stiftung (to B.M and K.K.). Work in the authors' laboratories is furthermore funded by grants from the DZHK (B14-013 (81X2800109), to O.N.U. and K.K.) and DFG (KL 595/2-3, to K.K.), from the Monika-Kutzner-Stiftung, the Else-Übelmesser-Stiftung, the Wilhelm-Sander-Stiftung, and the intramural graduate program "Mini-Graduiertenkolleg" of Tubingen University (to B.M.).

Conflict of interest

The authors declare no conflict of interest.

References

[1] J. Abe, Role of PKCs and NF-kappaB activation in myocardial inflammation: enemy or ally? J. Mol. Cell. Cardiol. 43 (2007) 404–408.
[2] J. Chen, Z. Wang, T. Wu, Shenqi fuzheng injection improves cvb3-induced myocarditis via inhibiting traf6 expression, Cell. Mol. Biol. (Noisy-le-grand) 59 (Suppl.) (2013) OL1826–OL1834.
[3] J.Y. Chung, M. Lu, Q. Yin, S.C. Lin, H. Wu, Molecular basis for the unique specificity of TRAF6, Adv. Exp. Med. Biol. 597 (2007) 122–130.
[4] M. Esfandiarei, S. Boroomand, A. Suarez, X. Si, M. Rahmani, B. McManus, Coxsackievirus B3 activates nuclear factor kappa B transcription factor via a phosphatidylinositol-3 kinase/protein kinase B-dependent pathway to improve host cell viability, Cell. Microbiol. 10 (2007) 2358–2371.
[5] K. Fuse, G. Chan, Y. Liu, P. Gudgeon, M. Husain, M. Chen, W.-C. Yeh, S. Akira, P.P. Liu, Myeloid differentiation factor-88 plays a crucial role in the pathogenesis of Coxsackievirus B3-induced myocarditis and influences type I interferon production,

Circulation 112 (2005) 2276–2285.
[6] J. Gui, Y. Yue, R. Chen, W. Xu, S. Xiong, A20 (TNFAIP3) alleviates CVB3-induced myocarditis via inhibiting NF-κB signaling, PLoS One 7 (9) (2012) e46515.
[7] Y.X. Ji, P. Zhang, X.J. Zhang, Y.C. Zhao, K.Q. Deng, X. Jiang, P.X. Wang, Z. Huang, H. Li, The ubiquitin E3 ligase TRAF6 exacerbates pathological cardiac hypertrophy via TAK1-dependent signalling, Nat. Commun. 7 (2016) 11267, http://dx.doi.org/10.1038/ncomms11267.
[8] Z. Jiang, M. Zamanian-Daryoush, H. Nie, A.M. Silva, B.R. Williams, X. Li, Poly(I-C)-induced Toll-like receptor 3 (TLR3)-mediated activation of NFkappa B and MAP kinase is through an interleukin-1 receptor-associated kinase (IRAK)-independent pathway employing the signaling components TLR3-TRAF6-TAK1-TAB2-PKR, J. Biol. Chem. 278 (2003) 16713–16719.
[9] R. Kandolf, M. Sauter, C. Aepinus, J.-J. Schnorr, H.-C. Selinka, K. Klingel, Mechanisms and consequences of enterovirus persistence in cardiac myocytes and cells of the immune system, Virus Res. 62 (1999) 149–158.
[10] K. Klingel, C. Hohenadl, A. Canu, M. Albrecht, M. Seemann, G. Mall, R. Kandolf, Ongoing enterovirus-induced myocarditis is associated with persistent heart muscle infection: Quantitative analysis of virus replication, tissue damage and inflammation, Proc. Natl. Acad. Sci. USA 89 (1992) 314–318.
[11] K. Klingel, R. Kandolf, The role of enterovirus replication in the development of acute and chronic heart muscle disease in different immunocompetent mouse strains, Scand. J. Infect. Dis. (Suppl. 88) (1993) 79–85.
[12] K. Klingel, M. Sauter, C.T. Bock, G. Szalay, J.J. Schnorr, R. Kandolf, Molecular pathology of inflammatory cardiomyopathy, Med. Microbiol. Immunol. 193 (2004) 101–107.
[13] K. Klingel, C. Fabritius, M. Sauter, K. Göldner, D. Stauch, R. Kandolf, N. Ettischer, S. Gahlen, T. Schönberger, S. Ebner, A.P. Makrigiannis, S. Bélanger, A. Diefenbach, B. Polić, J. Pratschke, K. Kotsch, The activating receptor NKG2D of natural killer cells promotes resistance against enterovirus-mediated inflammatory cardiomyopathy, J. Pathol. 234 (2014) 164–177.
[14] R. Ko, J.H. Park, H. Ha, Y. Choi, S.Y. Lee, Glycogen synthase kinase 3β ubiquitination by TRAF6 regulates TLR3-mediated pro-inflammatory cytokine production, Nat. Commun. 6 (2015) 6765, http://dx.doi.org/10.1038/ncomms7765.
[15] N.K. Lee, S.Y. Lee, Modulation of life and death by the tumor necrosis factor receptor-associated factors (TRAFs), J. Biochem. Mol. Biol. 35 (2002) 61–66.
[16] Z. Liu, H.M. Zhang, J. Yuan, T. Lim, A. Sall, G.A. Taylor, D. Yang, Focal adhesion kinase mediates the interferon-gamma-inducible GTPase-induced phosphatidylinositol 3-kinase/Akt survival pathway and further initiates a positive feedback loop of NF-κB activation, Cell. Microbiol. 10 (2008) 1787–1800.
[17] D. Marchant, X. Si, H. Luo, B. McManus, D. Yang, The impact of CVB3 infection on host cell biology, Curr. Top. Microbiol. Immunol. 323 (2008) 177–198.
[18] B. Munz, E. Hildt, M.L. Springer, H.M. Blau, RIP2, a checkpoint in myogenic differentiation, Mol. Cell. Biol. 22 (2002) 5879–5886.
[19] A. Riad, D. Westermann, C. Zietsch, K. Savvatis, P.M. Becher, S. Bereswill, M.M. Heimesaat, O. Lettau, D. Lassner, A. Dörner, W. Poller, M. Busch, S.B. Felix, H.P. Schultheiss, C. Tschöpe, TRIF is a critical survival factor in viral cardiomyopathy, J. Immunol. 186 (2011) 2561–2570.
[20] M. Saura, T.R. Lizarbe, C. Rama-Pacheco, C.J. Lowenstein, C. Zarazoga, Inhibitor of NF kappa B alpha is a host sensor of coxsackievirus infection, Cell Cycle 6 (2007) 503–506.
[21] Y. Song, W. Ge, H. Cai, H. Zhang, Curcumin protects mice from coxsackievirus B3-induced myocarditis by inhibiting the phosphatidylinositol 3 kinase/Akt/nuclear factor-κB pathway, J. Cardiovasc. Pharmacol. Ther. 18 (2013) 560–569.
[22] A.O. Weinzierl, G. Szalay, H. Wolburg, M. Sauter, H.G. Rammensee, R. Kandolf, S. Stevanović, K. Klingel, Effective chemokine secretion by dendritic cells and expansion of cross-presenting CD4-/CD8+ dendritic cells define a protective phenotype in the mouse model of coxsackievirus myocarditis, J. Virol. 82 (2008) 8149–8160.
[23] C. Zarazoga, M. Saura, E.Y. Padalko, E. Lopez-Rivera, T.R. Lizarbe, S. Lamas, C.J. Lowenstein, Viral protease cleavage of inhibitor of κBα triggers host cell apoptosis, Proc. Natl. Acad. Sci. USA 103 (2006) 19051–19056.
[24] H. Zhang, Y. Song, Z. Zhang, Glycyrrhizin administration ameliorates coxsackievirus B3-induced myocarditis in mice, Am. J. Med. Sci. 344 (2012) 206–210.
[25] Y. Zhang, W. Cao, Y.H. Xie, Q. Yang, X.Q. Li, X.X. Liu, S.W. Wang, The comparison of α-bromo-4-chlorocinnamaldehyde and cinnamaldehyde on coxsackie virus B3-induced myocarditis and their mechanisms, Int. Immunopharmacol. 14 (2012) 107–113.